Magnetotelluric profile across the Dabbahu magmatic segment, Afar, Ethiopia

Abstract

We have acquired high quality magnetotelluric (MT) and TEM (for static shift correction) data along a 50 km profile perpendicular to an active magmatic centre in Afar, Ethiopia. After robust processing, dimensionality and geoelectrical strike direction assessment, static shift correction and rotation into geoelectrical strike co-ordinates, the MT data have been inverted for a 2D model of resistivity beneath the profile, with a minimum misfit of 1.8. This model has a near surface conductor, interpreted as a sedimentary layer containing large quantities of saline fluid in the shallow sub-surface, and a deeper (lower crust/upper mantle) conductive zone, interpreted as a magma chamber or zone with significant partial melt. The data are being interpreted in conjunction with other geophysical, geological and remote sensing data to understand the processes associated with continental rupture.

Background

The Afar region of Ethiopia is slowly rifting to form a new ocean. Much of the associated deformation and volcanism is concentrated along elongated magmatic segments, where, at this late stage of continental break-up, strain is accommodated by injection and eruption of magma rather than seismically. Activity is episodic, and since late 2005 a number of events – volcanic eruptions, dyke injections and earthquake swarms – have profoundly affected the Dabbahu segment (Figure 1)[1-4]. It began in September 2005 with an explosive fissural eruption on the southern flanks of the Dabbahu volcano, opening a vent 500m long and 60m deep. An associated dramatic rifting event affected the entire 60km-long segment during which there were 163 earthquakes with magnitude >3.9, and over 8m of crustal movement[2,4]. A sequence of subsequent volcanic eruptions and dyke injections re-intruding the central and southern part of the rift has been documented[5], as activity has become concentrated in the Ado Ale Volcanic Complex (Figure 2). The 2005 event was caused by the dyke injection of around 2.5km^3 of magma in two weeks, more than was emplaced in over 10 years during the Krafla event on Iceland. The measured deflation of the Dabbahu and adjacent Gabho volcanoes is unable to account for this volume, even after allowing for degassing[1]. A further ~0.5km^3 has been intruded in later dyking events[5,21].

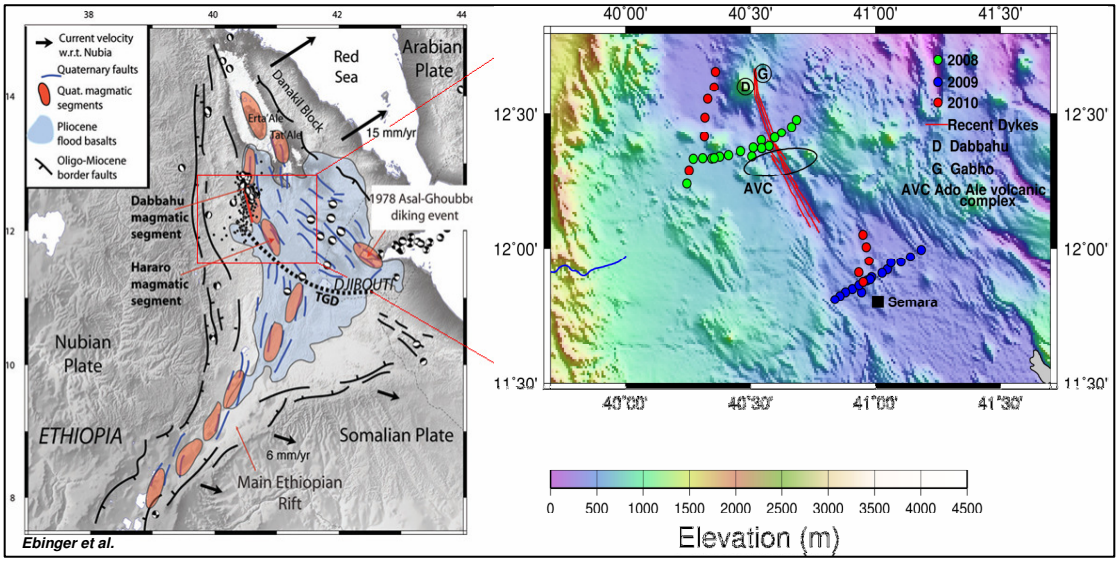

Figure 1. Tectonic setting of the area, after Ebinger et al. (2008)[4].

Figure 2. MT data acquired on the project, over the area of the red box in Figure 1. This report presents the results of the profile shown in green, though with the nearby red site replacing the most southerly green site.

An MT profile of 17 sites on a 50 km profile roughly perpendicular to the rift axis (Figure 2) follows and extends the line of GPS sites established in an earlier field campaign, and passes through a broadband seismometer location. Owing to the rugged topography, most sites were accessed by helicopter. Site spacing is roughly 5km over the majority of the profile, and ~3km over the rift axis where a more conductive regime, decreasing the skin depth, was expected. Most of the region is bare rock, and therefore site options were limited to where there were sufficiently large (~100m diameter) soil- or sand-covered patches to bury the electric and magnetic sensors; these were identified in advance from SPOT imagery and coordinates read off to give to the helicopter pilot. Data at the most westerly site of the profile were unusable at periods longer than 0.8s; therefore a replacement site was occupied in our 2010 field season. Data from all other sites were collected in 2008.

Survey procedure

Most sites were occupied for 24-36 hours, aiming to provide MT periods down to ~1000s. Equipment failure and electrode noise spikes restricted the maximum period to less than this at some sites. Non-polarising electrodes were placed in a salty, bentonite mud to provide good electrical contact. Magnetic coils were buried to reduce noise. We used a 'plus sign' configuration with electrode lines and coils orientated magnetic north-south and east-west. Electrode lines were about 100m long. We had 2-3 working sets of instruments at any one time, and at each site aimed to have synchronous recording with another site for part of the time to allow remote reference processing. Our main problem, besides noise spikes, was with battery power. Our sealed batteries were mislaid by Ethiopian Customs and the replacements were of much lower quality. In addition, a major sandstorm during the campaign meant that solar panels were not particularly effective at keeping batteries charged whilst deployed. We also had problems with sand and dust blowing into the systems, especially during the sandstorm, and with overheating in the high Afar temperatures.

At the majority of sites, we also collected TEM data for static shift control. After some experimentation, we ascertained that a square loop of dimensions 100 x 100m and effective receiver loop size of 31.4m^2 was optimum. The time rate of decay of magnetic flux was recorded over integration times from 0.25 to 120s. Data quality was uniformly good.

Processing and data quality

Data time series were robustly processed[6] to provide impedance tensor estimates. We used a variety of algorithms to investigate the dimensionality of the data, including phase tensor analysis[7]. Phase tensors ellipses by site and frequency are presented in Figure 3, from which it can be seen that a two-dimensional (2D) Earth approximation is adequate to explain most data, with departures mainly at short periods and beneath the rift axis. We used a variety of techniques to determine the geoelectrical strike direction, both on a site-by-site and period-by-period basis (see Figure 4) and using the 'strike' algorithm[8], which finds the optimum strike angle for all sites and periods. All analyses suggest the geoelectrical strike direction is ~340°; this is tectonically reasonable as it matches the rift axis orientation (Figures 1 and 2).

Static shift from galvanic distortion owing to small-scale, shallow conductors can lead to erroneous structure at all depths within MT models. Without independent control on the shallow structure such as provided by TEM data, the MT apparent resistivity (ρ_a) curve shifts are unknown. The TEM data were processed and modelled using Aarhus Geophysics SiTEM/Semdi software. The delay times from the processed TEM decay curves were turned into equivalent MT period[9]; curves were then matched to the actual MT ρ_a curves. The period overlap was small, but sufficient to determine static shifts in most cases. We found examples where both ρ_a MT curves needed shifting to match the TEM data curves, as well as the more usual situation where one or other mode ρ_a curve was moved up or down to match the other (see Figure 5).

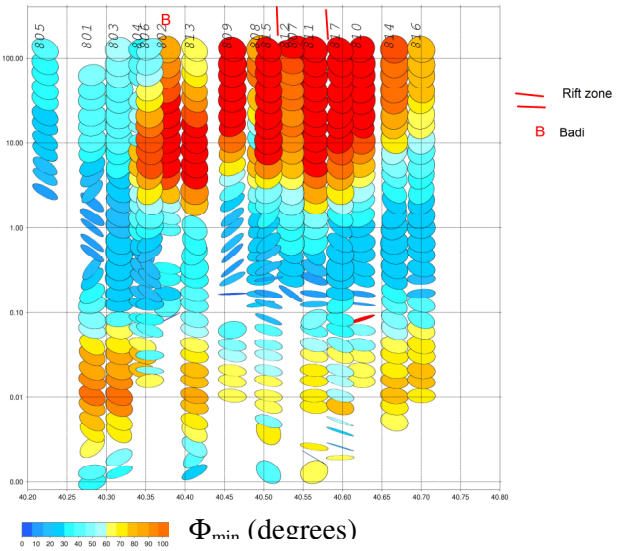

Figure 3 (left). Phase tensor ellipses[7] as a function of frequency (Hz). x-axis is longitude. The broadly circular ellipses are consistent with a 2D Earth.

Figure 4 (below). Rose histogram of phase tensor derived geoelectrical strike directions at all sites and all periods. Tick mark is 10 measurements.

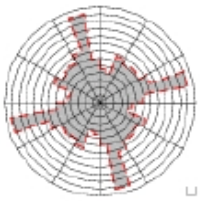

The MT data can also be corrected for static shift by solving for the parameters of an assumed distortion model while determining the electrical strike direction[8]; the results of the two methods agree well. The data were finally run through a ρ^+ consistency check[10]. Examples of the corrected and rotated data are presented as data pseudo-sections in Figure 6, and on a site-by-site basis in Figure 7. Of significant note are the low ρ_a values in both modes at most periods for sites over the rift axis, indicating a particularly conductive sub-surface. There is a second zone of less pronounced low ρ_a values about 15km to the west of the axis. The shape of the phase (φ) curves for both modes indicate a resistivity structure that increases initially and then decreases significantly with depth. Viewing the data on an individual site basis (Figure 7) shows the differences between the two modes more clearly. The period at which they separate is longer for ρ_a than φ; beyond that, TM mode ρ_a values tend to be lower, and φ values higher, than their TE counterparts. The low ρ_a features at the longest periods beneath the rift axis and centred on site 813 are much more pronounced in the TE mode, consistent with its greater sensitivity to conductive features at depth[13].

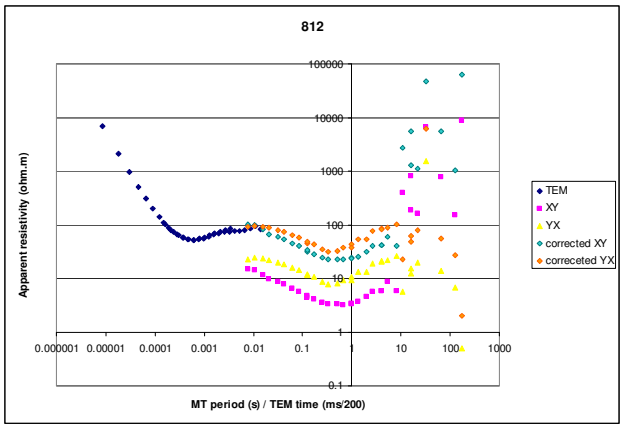

Figure 5. Example of static shift correction. TEM times are scaled down by a factor of 200[9]. This site (812) shows by far the largest amount of static shift out of all the sites for which we have TEM data. The static shift at other sites does not exceed 0.2 of a decade.

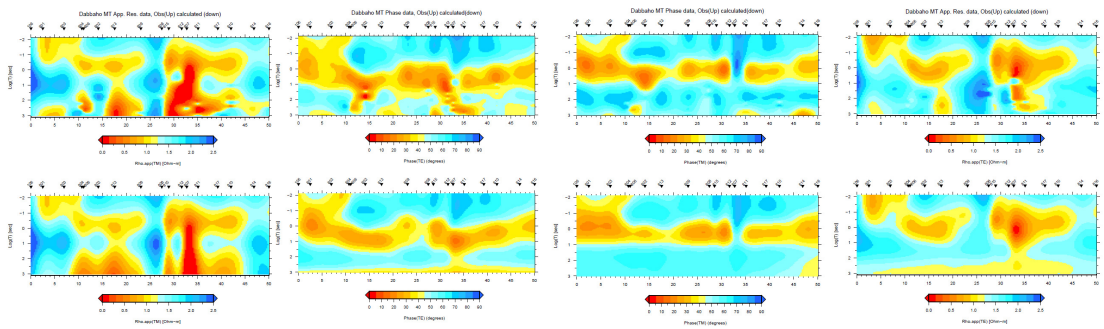

Figure 6 (above). Data pseudo-sections (top) and predictions of the model of Figure 8 (bottom). TM ρ_a, φ, TE ρ_a, φ, from left to right.

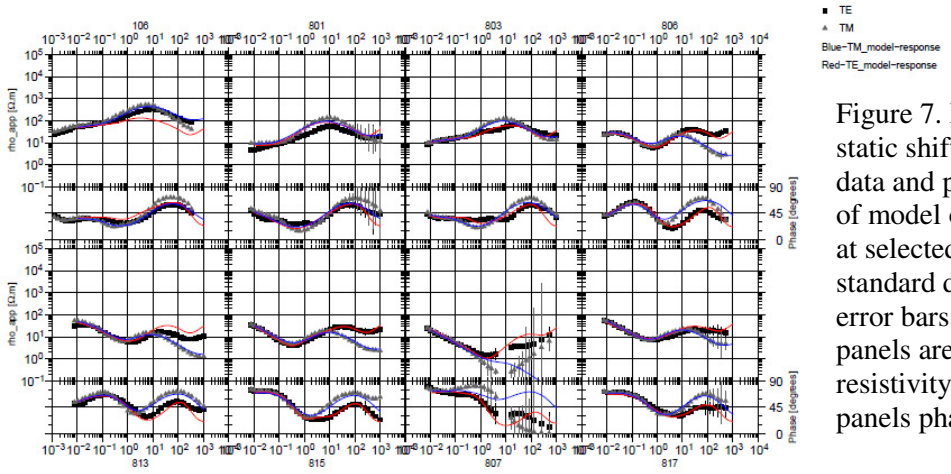

Figure 7. Rotated, static shift-corrected data and predictions of model of Figure 8 at selected sites. One standard deviation error bars. Top panels are apparent resistivity, lower panels phase.

Modelling

A 2D model space was parameterised into blocks of constant resistivity, with a variable block size represented the decreasing resolution of the data with depth and the site distribution, following accepted guidelines. The mesh contained 125 vertical and 35 horizontal divisions, covering an area of 220 x 60 km. In addition, there were 10 air layers. The resistivities of these 4375 blocks were determined from 2063 TE and TM data (up to 35 periods per site ranging from 0.0078 s to 1024 s) using the 2D REBOCC algorithm[11]. Only the area below the profile is presented here, to a depth of 30 km, the maximum resolved by the data (as determined by sensitivity tests).

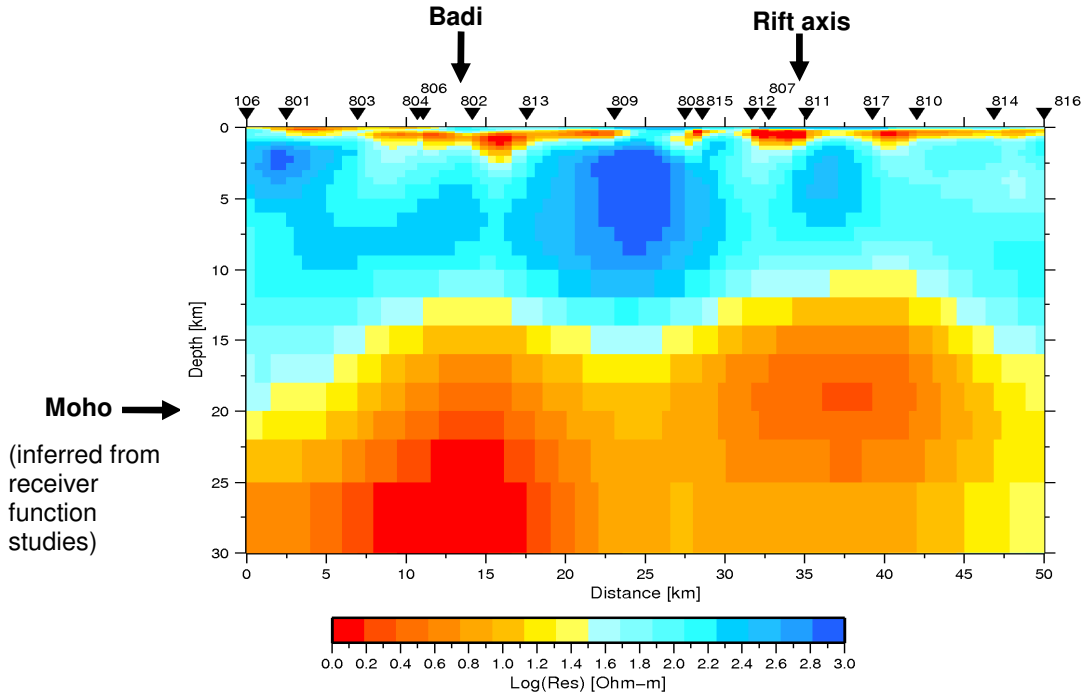

Figure 8. 2D inversion result obtained by joint inversion of the TE and TM modes, iterating from a uniform half space.

A number of inversions were performed to assess the reliability of the solution and the 2D model fit. The main model features are robust, and describe well the data at periods at which the 2D assumption holds. The model shown in figure 8 is our preferred inversion of the 'strike' analysed distortion-corrected data, iterating from a uniform half-space model. The overall root-mean-square misfit is 1.8. Predictions of the model are shown in Figure 6 as pseudo-sections and superimposed on the data curves of Figure 7.

Interpretation to date and preliminary findings

The model (Figure 8) shows exceptionally high conductivity throughout the deep crust and upper mantle, beginning at about 10 km depth. It has two maxima, shallower below the rift axis, and in the upper mantle (receiver function studies show the Moho is at around 20 km depth; J Hammond, pers. comm., 2009) to the west, beneath sites adjacent to the Badi volcano. The base of the crust and upper mantle between them is less conductive, with the slightly higher resistivity well-characterised by the longer period data at sites 809 and 815. High mantle conductivities are required to fit the data at many sites, extending to their maximum penetration depth. Whether the mantle conductor continues to the east of the rift axis is uncertain, since the data there do not extend to sufficiently long periods. At these depths, such high values can only be caused by material in a fluid or partially molten phase, here assumed to be the magma that we know is associated with the observed rifting, dyke injections and eruptions.

An unexpected feature of the resistivity structure is the almost ubiquitous shallow conducting layer, with variable thickness but between about 500 m and 2 km depth. Such high conductivities in the near surface are likely to be caused by saline fluids in sediments. Rock samples collected from the Dabbahu volcano and the Ado Ale Volcanic Complex show evidence for fractionation in the presence of brines (C. Ebinger, pers. comm., 2010). Support for a substantial thickness of sediments comes from large delays in receiver functions (J. Hammond, pers. comm., 2009) similar to those seen in the northern main Ethiopian rift[12], where sedimentary thicknesses were interpreted from controlled source seismic data unavailable in Afar.

The MT results constrain the amount of melt in the deeper conductor. Its high conductivity indicates well-connected melt within a solid rock matrix. In Afar we have strong indications that the sub-surface is anisotropic[13,14], caused at these depths by oriented melt pockets[15]. In this case, melt is connected along parallel pathways, giving a slightly lower melt fraction than the Hashin-Shtrikman upper bound[16] for the same bulk conductivity[17]. Our deeper conductor has conductance values in the range 2000 - >40,000 S. Taking an indicative solid rock resistivity of 2000 Ωm[18] and basaltic melt value of 0.1 Ωm[19] suggests ~6% melt, based on an average resistivity of 1.8 Ωm from a typical conductance value and 15 km thickness. Note that this is still much larger than values of a fraction of a percent needed to explain seismic anisotropy data with oriented melt pockets[13-15].

Seismic v_P/v_S ratios of around 2.1 (J. Hammond, pers. comm., 2009) support the existence of large quantities of melt. The lack of good arrivals for receiver function studies is consistent with attenuation by abundant melt. Best-fitting models of post-dyking viscoelastic relaxation of GPS and other data have a crust of 12-14 km effective elastic thickness over a viscoelastic layer of viscosity ~5×10^{18} Pa s[20]; this is considerably less than typical upper mantle viscosities and thus indicative of the presence of melt. Although the seismic data suggest part of the visco-elastic layer is crustal, all techniques, including MT, are in agreement that it contains large amounts of melt. Predominantly basaltic eruptions indicate mantle-derived melt, in agreement with our conclusion that part of the magma chamber is located in the mantle. inSAR data modelling[21] puts a deep (Mogi) source at 25 km beneath the mid-segment, consistent with our maximum conductivity at depths of 27-30 km, given that the inSAR source depth is poorly constrained and strongly dependent on geometry.

Conclusions and further work

MT with TEM for static shift control and robust processing has produced an excellent data set in the harsh and difficult conditions of Afar. 2D inversion indicates large areas of high conductivity in the sub-surface beneath the Dabbahu magmatic segment. The data can be reconciled with those from other studies and provide the first direct evidence for a deep magma chamber, indicated by its high electrical conductivity.

Further work will include analysis of the variation of geoelectrical strike with period and comparisons with variations in seismic anisotropy amounts and fast directions with depth. In addition, 3D modelling indicates a variable depth to the top of the deep-crustal conductor to the north and south of the profile, which will be correlated with inSAR data models[5].

We have also collected other MT and TEM data in the area (Figure 2), and the results of the later field campaigns will be compared and integrated with those presented here. BGR, Germany have collected MT data in an adjacent area to the south for geothermal studies; we are sharing data with them and will liaise on interpretation.

References [1]Wright, T J, et al., 2006, *Nature,* **442,** 291–294; [2]Rowland, J V, et al., 2007, *Geophys. J. Int.,* **171,** 1226–1246; [3]Keir, D, *et al.*, 2009, *Geology,* **37**, 59–62. [4]Ebinger, C J, et al., 2008, *Geophys. J. Int.,* **174**, 1138–1152. [5]Hamling, I J, et al., 2009, *Geophys. J. Int.,* **178**, 989-1003; [6]Chave A D and Thomson D J, 1989, *J. Geophys. Res*., **94**, 14215- 14225; [7]Caldwell T G, et al., 2004, *Geophys. J. Int.,* **158**, 457-469; [8]McNeice, G W and Jones, A G, 2001, *Geophysics*, **66**, 158-173; [9]Sternberg, B, et al., 1988, *Geophysics*, **53**, 1459-1468; [10]Parker, R L and Booker, J R, 1996, *Phys. Earth Planet. Ints.*, **98**, 269-282; [11]Siripunvaraporn, W and Egbert, G, 2000, *Geophysics*, **65**, 791-803; [12]Cornwell, DG, et al., 2010, *Geochem. Geophys. Geosys.*, Q0AB03, doi: 10.1029/2009GC002637; [13]Kendall J M, et al., 2005, *Nature*, **433**, 146-148; [14]Kendall J M, et al., 2006, *Geol. Soc. Lond. Sp. Publ*., **259**, 55-72; [15]Bastow I D, et al., 2010, *Geochem. Geophys. Geosys.*, **11**, Q0AB05, doi:10.1029/2010GC003036; [16]Hashin, Z and Shtrikman, S, 1962, *J. Appl. Phys.*, **33**, 3125-3131; [17]Roberts, J J and Tyburczy, J A, 1999, *J. Geophys. Res.*, **104**, 7055-7065; [18]Li, S, et al, 2003, *Geophys. J. Int.*, **153**, 289-304; [19]Yoshino, T, et al., 2010, *Earth Planet. Sci. Lett.*, **295**, 593–602; [20]Norris, S, et al., E, 2009, *Geophys. Res. Lett.*, **36**, L21308, doi:10.1029/2009GL040502; [21]Grandin, R, et al., 2010, *J. Geophys. Res.*, **115**, B09403, doi:10.1029/2009JB006883

Publications

Desissa, M, 2010. Magnetotelluric Survey in the Dabbaho Volcanic Segment, Afar Depression, Northern Ethiopia, unpublished MSc dissertation, University of Edinburgh (awarded with Distinction)

Desissa, M *et al.*, 2010. Journal paper in preparation.

Fisseha, S, Desissa, M, Johnson, N, Hautot, S, Whaler, K, Dawes G and Haile, T, 2010. Locating magma in Afar, Ethiopia – Magnetotelluric studies, abstract for the 20th IAGA WG 1.2 Workshop on Electromagnetic Induction in the Earth

Hautot, S, Whaler, K A, Desissa, M, Dawes, G, Fisseha, S and Johnson N, 2009. 3-D Conductivity structure of an active magmatic segment associated with the final stage of continental break-up: Afar, Ethiopia, *Eos Trans. AGU,* ***90*****(52)**, Fall Meet. Suppl., Abstract T43F-07

Johnson, N, Whaler, K, Hautot, S, Desissa, M, Fisseha, S, Dawes G and the rest of the Afar Consortium team, 2010. Magnetotellurics as part of an inter-disciplinary study of late-stage continental rifting in Afar, Ethiopia, abstract for the 20th IAGA WG 1.2 Workshop on Electromagnetic Induction in the Earth

Acknowledgement This GEF loan was supplemented by equipment loaned from the Geophysical Instrument Pool Potsdam (part of GeoForschungsZentrum)